Interactions of bile salts with a dietary fibre, methylcellulose, and impact on lipolysis

Interactions of bile salts with a dietary fibre, methylcellulose, and impact on lipolysis

Olivia Pabois[a, b], Amandine Antoine-Michard[a], Xi Zhao[b], Jasmin Omar[b], Faizah Ahmed[b], Florian Alexis[a], Richard D. Harvey[c], Isabelle Grillo[a], Yuri Gerelli[a], Myriam M.-L. Grundy[d], Balazs Bajka[e], Peter J. Wilde[f], Cécile A. Dreiss[b*]

[a] Institut Laue-Langevin, Grenoble 38000, France

[b] Institute of Pharmaceutical Science, King's College London, London SE1 9NH, United-Kingdom

[c] Institut für Pharmazie, Martin-Luther-Universität Halle-Wittenberg, Halle (Saale) 06099, Germany

[d] School of Agriculture, Policy and Development, University of Reading, Reading RG6 6AR, United-Kingdom

[e] Department of Nutritional Sciences, King's College London, London SE1 9NH, United-Kingdom

[f] Quadram Institute Bioscience, Norwich Research Park, Norwich NR4 7UA, United-Kingdom

E-mail addresses:

olivia.pabois@kcl.ac.uk; amandine-03@hotmail.fr; xi.zhao@kcl.ac.uk; jasmin.1.omar@kcl.ac.uk; faizah.ahmed@kcl.ac.uk; floalexis0@gmail.com; richard.harvey@pharmazie.uni-halle.de; grillo@ill.fr; gerelli@ill.fr; m.m.grundy@reading.ac.uk; balazs.bajka@kcl.ac.uk; peter.wilde@quadram.ac.uk; cecile.dreiss@kcl.ac.uk

Corresponding author:

Cécile A. Dreiss:

King's College London
Institute of Pharmaceutical Science
Franklin-Wilkins Building

150 Stamford Street
SE1 9NH London, UK
Tel: +44 (0)207 848 3766

Highlights

- BS, NaTC and NaTDC, impact the rheological properties and gelation of MC.
- NaTDC has a greater impact on the viscoelasticity of MC compared to NaTC.
- NaTDC desorbs from a MC-stabilised interface at lower concentrations than NaTC.
- Upon digestion, NaTDC destabilises more readily MC-stabilised emulsion droplets.
- During MC-stabilised emulsion digestion, NaTDC generates less FFA than NaTC.

Abstract

Methylcellulose (MC) has a demonstrated capacity to reduce fat absorption, hypothetically through bile salt (BS) activity inhibition. We investigated MC cholesterol-lowering mechanism, and compared the influence of two BS, sodium taurocholate (NaTC) and sodium taurodeoxycholate (NaTDC), which differ slightly by their architecture and exhibit contrasting functions during lipolysis.

BS/MC bulk interactions were investigated by rheology, and BS behaviour at the MC/water interface studied with surface pressure and ellipsometry measurements. *In vitro* lipolysis studies were performed to evaluate the effect of BS on MC-stabilised emulsion droplets microstructure, with confocal microscopy, and free fatty acids release, with the pH-stat method.

Our results demonstrate that BS structure dictates their interactions with MC, which, in turn, impact lipolysis. Compared to NaTC, NaTDC alters MC viscoelasticity more significantly, which may correlate with its weaker ability to promote lipolysis, and desorbs from the interface at lower concentrations, which may explain its higher propensity to destabilise emulsions.

Keywords

Methylcellulose; bile salts; rheology; surface pressure measurements; *in vitro* duodenal lipolysis

Graphical abstract

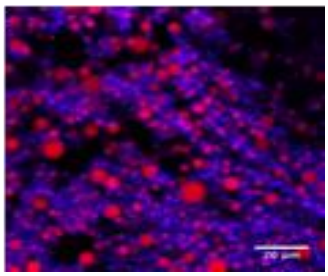

Oil droplets stabilised by methylcellulose

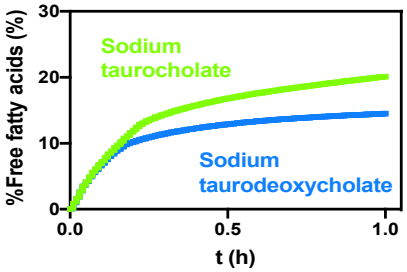

Methylcellulose-stabilised emulsion *in vitro* digestion

1. Introduction

Obesity and associated health risks (such as chronic cardiovascular diseases and type-2-diabetes mellitus) have become increasingly prevalent worldwide. In 2016, 39% of the world's adult population were classified as overweight, and 13% as obese (World Health Organization, 2019). Controlling the digestion of dietary lipids (fats) and optimising their absorption are therefore crucial to addressing this ongoing health crisis (McClements & Li, 2010b; Mei, Lindqvist, Krabisch, Rehfeld, & Erlanson-Albertsson, 2006). With their demonstrated capability to reduce food intake and aid weight loss, dietary fibres have shown great potential against obesity (Slavin, 2005). Nonetheless, a better understanding of the processes responsible for their ability to regulate calorie uptake still needs to be provided. Due to its approved (Younes et al., 2018) and wide (The Dow Chemical Company, 2002) use in the food industry, as well as its proven capacity to diminish blood cholesterol levels (without inducing any adverse effect) (Agostoni et al., 2010), methylcellulose (MC) is an appropriate model of dietary fibre for elucidating the mechanism by which dietary fibres reduce hyperlipidaemia.

MC is a non-ionic polysaccharide belonging to the large family of cellulose ethers and containing repeating anhydroglucose units, with methyl (hydrophobic) moieties substituting hydroxyl (hydrophilic) groups (Nasatto et al., 2015b) (Figure 1). The capacity of this dietary fibre to hinder lipolysis has been mainly attributed to its ability to induce loss of bile salts (BS) and cholesterol in faeces by (i) increasing the viscosity of the small intestine content (Christos Reppas, Meyer, Sirois, & Dressman, 1991), which slows down fat digestion and reduces nutrients absorption (Bartley et al., 2010; Carr, Gallaher, Yang, & Hassel, 1996; Maki et al., 2009; C. Reppas, Swidan, Tobey, Turowski, & Dressman, 2009; van der Gronde, Hartog, van Hees, Pellikaan, & Pieters, 2016), and/or by (ii) trapping BS and/or cholesterol molecules in its network, *via* hydrophobic interactions occurring both in the bulk aqueous phase and at the fat droplet interface (Pilosof, 2017; Pizones Ruiz-Henestrosa, Bellesi, Camino, & Pilosof, 2017; Torcello-Gómez et al., 2015; Torcello-Gómez & Foster, 2014). BS are biosurfactants produced in the liver and released into the small intestine (duodenum) (Hofmann & Mysels, 1987), which play key roles in lipid digestion and absorption (Maldonado-Valderrama, Wilde, Macierzanka, & Mackie, 2011; Wilde & Chu, 2011): on the one hand, they facilitate enzyme adsorption to fat droplet interfaces, thus promoting enzyme-catalysed lipolysis (Borgström,

Erlanson-Albertsson, & Wieloch, 1979; Bourbon Freie, Ferrato, Carrière, & Lowe, 2006; Erlanson-Albertsson, 1983; Labourdenne, Brass, Ivanova, Cagna, & Verger, 1997); on the other, they remove the enzyme-inhibiting insoluble lipolysis products (diacylglycerols (DAG), monoacylglycerols (MAG) and free fatty acids (FFA)) present at the interface, carrying them to the gut mucosa for absorption (Hofmann & Mysels, 1987). In this work, we are focusing on the interactions between MC and BS, which have been hypothesised to explain (i) MC cholesterol-lowering effect, due to the reduction in BS re-absorption in the ileum and the subsequent increased production of BS by the liver from cholesterol, and (ii) the early signalling of satiation and lengthening of satiety feeling, by the accumulation of undigested materials in the duodenum, due to BS being entrapped and prevented from fulfilling their functions during lipolysis (Gunness & Gidley, 2010). Recent studies have demonstrated BS inhibitory effect on MC thermally-induced structuring using microcalorimetry and rheology (Torcello-Gómez et al., 2015; Torcello-Gómez & Foster, 2014), and the competition of BS with MC for adsorption at the lipid droplet/water interface with tensiometry (Torcello-Gómez & Foster, 2014). However, there is little structural evidence for the hypothesis of entrapment of BS by MC, and a mechanistic understanding of the competitive processes leading to enzyme inhibition, delayed fat digestion and the associated health benefits, is still lacking. Therefore, further studies are required to clarify how MC interacts with BS during lipid digestion and how this, in turn, correlates to BS molecular structure and their contrasting roles.

The work presented here increases our understanding of the mechanisms underlying MC capacity to regulate fat digestion in the small intestine, with a particular focus on its ability to compete with BS for adsorption at the lipid droplet/water interface. More specifically, by combining bulk and interfacial experiments with *in vitro* lipolysis studies, we examined the interactions between MC and BS in bulk water, at the MC/water interface, and at the oil/water interface of fat droplets mimicking food colloids. It has been hypothesised that BS structural diversity is responsible for the different functions they carry out in fat digestion; to explore this postulate, two BS, sodium taurocholate (NaTC) and sodium taurodeoxycholate (NaTDC) (Figure 2), were selected, as they display contrasting adsorption/desorption dynamics, which are thought to reflect their different roles in the gut (Pabois et al., 2019; Parker, Rigby, Ridout, Gunning, & Wilde, 2014). Since BS are expected to interact with MC both in the bulk aqueous phase and at the surface of MC-stabilised emulsion droplets, we assessed the impact of BS on MC rheological properties, using oscillatory shear rheology, and BS/MC interfacial behaviour

120 at the air/water interface, through surface pressure measurements in a Langmuir trough set-
121 up and ellipsometry. We then investigated how these interactions affect the lipolysis of an
122 MC-stabilised emulsion, by monitoring the structure of emulsion droplets after addition of BS
123 and enzymes, with different optical microscopy techniques, and by measuring the amount of
124 FFA released throughout *in vitro* lipid digestion, with the pH-stat method.
125

2. Experimental section

2.1 Materials

Methocel™ SG A7C (solution viscosity: 700 mPa.s at 2% w/w at 20°C; methoxyl degree of substitution: 1.8; molecular weight: 400 - 500 kDa) (Figure 1) was kindly supplied by Dow Wolff Cellulosics GmbH (Bomlitz, Germany). Chloroform ($CHCl_3$) was purchased from Fisher Scientific (Loughborough, UK). NaTC (P97.0% TLC) (Figure 2A), NaTDC (P95.0% TLC) (Figure 2B), paraffin oil, ethanol (EtOH, P99.8% GC), orlistat (P98.0%), Nile red, fluorescent brightener 28 (calcofluor), dimethyl sulfoxide anhydrous (P99.9%), sunflower seed oil from *Helianthus annuus*, pancreatin from porcine pancreas (or pancreatic lipase/co-lipase; activity: 40 U/mg of solid, based on lipase activity using tributyrin as a substrate), sodium phosphate monobasic dihydrate (NaH_2PO_4, P99.0% T), sodium phosphate dibasic dihydrate (Na_2HPO_4, P99.0% T), sodium chloride (NaCl, P99.8%), calcium chloride dihydrate ($CaCl_2$, P99.0%) and sodium hydroxide (NaOH, 0.1 M) were all obtained from Sigma-Aldrich (Gillingham, UK). Ultrapure water, or MilliQ-grade water (H_2O, 18.2 MΩ·cm, Merck Millipore, Molsheim, France), was used in all experiments. Phosphate buffer (10 mM, pH = 7.04 at 21°C) was prepared by mixing 0.01% wt NaH_2PO_4 with 0.01% wt Na_2HPO_4, in ultrapure water. All reagents were used as supplied.

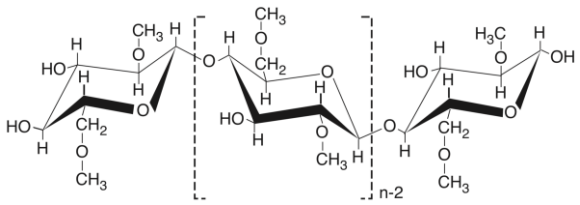

Figure 1: Structure of methylcellulose (MC)

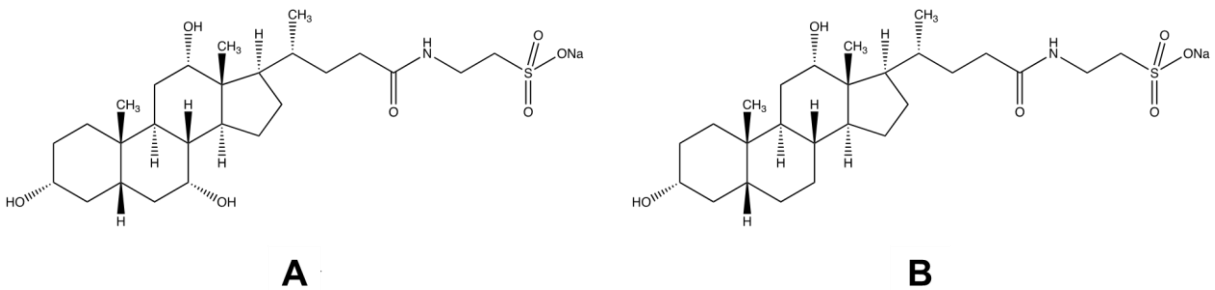

Figure 2: Structures of sodium taurocholate (NaTC) (A) and sodium taurodeoxycholate (NaTDC) (B)

2.2 Methods

2.2.1 Bulk and interfacial studies

2.2.1.1 Preparation of MC and MC/BS aqueous solutions

MC aqueous solution was prepared using the "hot/cold" method (The Dow Chemical Company, 2002, 2013). Solid MC was first dispersed into one third of the required mass of ultrapure water heated to 80°C (for around 15 minutes), until complete wetting of particles; then, the dispersion was transferred into an ice bath, and the remaining two thirds of cold ultrapure water (4°C) were added progressively into the stirred solution, which was finally left to stir overnight at 4°C, to ensure complete solubilisation. MC/BS solutions were prepared simply by mixing both components together at the required concentrations.

2.2.1.2 Rheology measurements

Rheology experiments were performed with a strain-controlled rheometer (ARES, TA instruments, Inc, Borehamwood, UK), fitted with a 25 mm diameter titanium parallel plate and equipped with a temperature-controlled Peltier system (with a $\pm$ 0.1°C temperature stability at thermal equilibrium). Each sample was loaded onto the lower plate, and the upper plate was adjusted to a gap size of 0.8 $\pm$ 0.3 mm. A thin layer of low viscosity paraffin oil was deposited around the edges of the sample exposed to air to prevent sample drying and evaporation throughout the measurement.

Dynamic temperature sweeps were performed at a fixed angular frequency of 6.28 rad/s and strain of 1%, from 20°C to 80°C, with a heating rate of 2°C/min, to measure the evolution of the storage (*G'*) and loss (*G''*) moduli as a function of temperature, in the absence and presence of BS. Dynamic frequency sweeps were performed over an angular frequency range of 0.1 - 100 rad/s, at a fixed strain of 1%, and a fixed temperature of 60°C (above MC transition temperature (T_t), which is the point where a break in the slope of *G'* is detected in the dynamic temperature sweep curves). The strain of 1% was chosen within the linear viscoelastic regime, which was established by performing dynamic strain amplitude sweeps on MC and MC/BS solutions, over a strain range of 0.01 - 100%, at a constant angular frequency of 6.28 rad/s and a temperature of 60°C. Each test was repeated at least twice to confirm reproducibility; representative curves (rather than averages) are shown in the manuscript.

2.2.1.3 Langmuir trough measurements

Interfacial tension measurements were performed in a 50 mm diameter perfluoroalkoxy Petri dish (19.6 cm^2 surface area and 20 mL volume of subphase), to study the adsorption of MC and its interaction with BS at the air/water interface. All experiments were carried out under constant stirring, at a fixed area, and at a temperature of 23 ± 2°C (room temperature). The surface pressure (π) was measured by a Wilhelmy plate made of chromatographic paper (Whatman International Ltd, Maidstone, UK) of 2.3 x 1.0 cm (length x width) and attached to a calibrated Nima PS4 microbalance (Nima Technology Ltd, Coventry, UK). Prior to any measurement, the trough was thoroughly cleaned with EtOH and $CHCl_3$ to remove organic impurities, and then filled with ultrapure water (subphase). Surface-active contaminants, dust and bubbles were all removed from the subphase by suction with a pump, and the subphase was considered as clean when changes in surface pressure did not exceed ± 0.2 mN/m over approximately two minutes.

MC adsorption at the air/water interface. Using a 1 mL syringe (Becton Dickinson, Madrid, Spain) fitted with a 19 G x 1 ½ in. needle (Becton Dickinson, Madrid, Spain), a specific amount of pure MC solution in ultrapure water was injected into the subphase, under constant stirring. Surface pressure (π) was measured over time until it reached a plateau. Each experiment was repeated at least twice; either a representative curve or an average measurement is shown.

BS interaction with a MC layer at the air/water interface. A MC layer was first formed at the air/water interface, by addition of a specific amount of MC aqueous solution into the clean and stirred water (π_{MC} = 21 ± 1 mN/m with 0.5‰ w/w, and π_{MC} = 18 ± 2 mN/m with 0.5×10^{-2}‰ w/w). After film equilibration (ca. 1-2 hours), a specific amount of pure BS aqueous solution was injected beneath the MC layer. The corresponding changes in surface pressure (π) were recorded over time. Each experiment was repeated at least twice; either a representative curve or the average measurement is shown.

2.2.1.4 Ellipsometry

MC adsorption and interaction with BS at the air/water interface was further investigated by ellipsometry (Beaglehole Instruments, Wellington, New Zealand). Time-dependent measurements were performed with a 632.8 nm-wavelength laser hitting the surface at an incident angle of 50°. In this configuration, changes in the polarisation of light reflected by the

interface are measured over the 1 mm² area and ~1 µm depth probed by the laser beam; these changes can be correlated to the amount of material adsorbed at this interface over time. The polarisation state of the incident light is composed of an *s*- and *p*-component (where the *s*-component is oscillating parallel to the sample surface, and the *p*-one parallel to the plane of incidence). The ratio of the reflectivity of these two components (r_s for the *s*-component and r_p for the *p*-component) characterises the polarisation change and is expressed by the following equation:

$$\frac{r_p}{r_s} = \tan(\Psi).\, e^{i\Delta} \qquad (1)$$

where Ψ is the amplitude change and Δ the phase shift. In the thin film limit at the air/water interface (i.e., film thickness << laser wavelength), Δ is found to be much more sensitive to changes in the amount adsorbed at the interface than Ψ (Motschmann & Teppner, 2001). Therefore, time-dependent changes in phase shift ($\Delta\Delta$) were measured, with $\Delta\Delta(t) = \Delta(t) - \Delta(t_0)$, where $\Delta(t_0)$ is the phase shift at the beginning of a given experiment, namely, the phase shift of the bare air/water interface (Δ_0) for MC adsorption and interaction with BS, at the air/water interface. Changes in the phase shift are directly proportional to the amount of material adsorbed at the interface (Motschmann & Teppner, 2001). In order to measure simultaneously the surface pressure and phase shift for the same surface, the instrument was mounted on top of the Petri dish, used as a Langmuir trough. Data were acquired at a rate of 0.2 Hz, using the Igor Pro software.

2.2.2 *In vitro* lipolysis studies

2.2.2.1 Preparation of MC-stabilised emulsion

MC (0.5% w/w) was dispersed into sunflower oil (15% w/w). Cold phosphate buffer (84.5% w/w, at $T < T_{dissolution}$ = 10°C) was added to the oil phase and the mixture stirred for a few minutes. The dispersion was then pre-emulsified at 11,000 rpm for 1 minute, using a high-shear mixer (T25 digital Ultra-Turrax, IKA®-Werke GmbH & Co. KG, Staufen, Germany). This pre-emulsion was transferred into a 10 mL volume beaker in an ice bath and was sonicated at a frequency of 20 kHz and amplitude of 70% for 5 minutes with a tip sonicator (SONOPULS HD 3100 ultrasonic homogeniser, microtip model: MS 73, BANDELIN electronic GmbH & Co. KG, Berlin, Germany).

2.2.2.2 Simulation of the duodenal lipolysis environment

For each *in vitro* lipolysis experiment, the following model (Grundy, Wilde, Butterworth, Gray, & Ellis, 2015) was employed to simulate the duodenum (small intestine) environment: 19 mL of MC-stabilised emulsion was added to a thermostatically-controlled and mechanically-stirred reaction vessel at 37°C, followed by 15 mL of a BS aqueous solution (NaTC, NaTDC; 2.5, 25, 125 mM, in phosphate buffer). Then, 1 mL of NaCl (4.9 M, in ultrapure water) and 1 mL of $CaCl_2$ (0.37 M, in ultrapure water) were added to the mixture, under continuous stirring. Finally, 1.5 mL of either phosphate buffer (for the blank assay, used as a control) or freshly prepared pancreatic lipase/co-lipase suspension (17 mg/mL, in phosphate buffer) (for the lipolysis assay) were added. The final system was made up of 7.6% w/w lipid, 1, 10, or 50 mM BS, 130 mM NaCl, 10 mM $CaCl_2$, and 0.68 mg/mL pancreatic lipase/co-lipase.

2.2.2.3 Optical microscopy

The structural changes induced on an MC-stabilised emulsion upon duodenal digestion, were monitored over time by brightfield optical (Olympus BX61 microscope, Olympus France S.A.S., Rungis, France) and confocal (Leica TCS SP2, DMIRE2 inverted, Leica Microsystems UK Ltd, Milton Keynes, UK) microscopy. Prior to *in vitro* lipolysis studies, the pure emulsion was characterised; then, the mixture modelling the duodenal environment was added to the emulsion and samples measured at different time points (t = 5, 15, 30 and 60 min), to analyse the evolution of emulsion droplet microstructure from the beginning to the end of duodenal lipolysis. The influence of each component (NaTC, NaTDC, NaCl and $CaCl_2$) used individually and together was assessed to better understand their impact on duodenal lipolysis. A blank assay was also measured as a control to monitor changes over time in the absence of enzymes.

For confocal microscopy, prior to visualisation, samples were mixed with 1 mg/mL orlistat (prepared in dimethyl sulfoxide) to stop lipolysis, and then stained with 10 µg/mL Nile red (prepared in dimethyl sulfoxide) and 20 µg/mL calcofluor (prepared in ultrapure water), to detect lipids (red fluorescence) and MC (blue fluorescence), respectively. Samples were excited at 488 nm (for Nile red) and 405 nm (for calcofluor), and the fluorescence emitted by the samples was detected between 510 - 650 nm (for Nile red) and 410 - 480 nm (for calcofluor). Images were captured using objective lenses of 10×, 20× or 63×, and micrographs

were compiled with the Olympus image analysis software (for optical microscopy, Olympus France S.A.S., Rungis, France) and Fiji software ("Fiji," 2019) (for confocal microscopy).

2.2.2.4 pH-stat measurements

The rate and extent of lipolysis were evaluated by titrating the amount of FFA released from an MC-stabilised emulsion with 0.1 M NaOH, at 37°C and pH 7.0, in conditions mimicking the duodenal (small intestine) environment. Each assay was carried out over 1 hour of digestion, using a pH-stat titration unit (848 Titrino plus, Metrohm AG, Herisau, Switzerland). The blank experiment was performed as a control, to measure pH fluctuation in the absence of enzymes; the volume of NaOH released during this assay was then subtracted from the data recorded in the presence of pancreatic lipase/co-lipase (lipolysis assay). Each blank and lipolysis experiment was repeated at least six times.

The volume of NaOH released during MC-stabilised emulsion digestion was converted into the percentage of FFA produced, using this equation:

$$\%\text{FFA (t)} = 100 \times \frac{V_{NaOH}\,(t)\,.\,[NaOH]\,.\,M_{Lipid}}{2\,.\,m_{Lipid}} \quad (2)$$

where V_{NaOH} is the volume of NaOH required to neutralise the FFA produced over time, *[NaOH]* the concentration of the NaOH solution used, M_{Lipid} the molecular weight of the oil employed in this experiment (in our case, $M_{Sunflower\ oil}$ = 876 g/mol (Sánchez, Maceiras, Cancela, & Rodríguez, 2012)), and m_{Lipid} the mass of triacylglycerol (TAG) initially present in the digestion vessel. This equation has been established considering the ideal case where the hydrolysis of one molecule of TAG leads to the formation of one molecule of MAG and two molecules of FFA. The results are shown as the proportion of FFA release as a function of time.

The pH-stat data were analysed with the GraphPad Prism software ("GraphPad Prism," 2019); statistical analysis was carried out using the two-way analysis of variance (ANOVA), followed by the Tukey post-test, with a 95% confidence level, meaning that differences were considered as statistically significant when $P < 0.05$.

3. Results

3.1 BS interaction with MC in the bulk

MC viscoelastic behaviour. The temperature-dependence of MC rheological properties was investigated by performing dynamic temperature sweep measurements on MC solutions prepared at concentrations ranging between 0.1 and 2.0% w/w (Figure S1).

At all the MC concentrations studied, a relatively flat region is observed for the storage modulus (*G'*) in the lower temperature range (ca. 20 - 40°C), followed by a steep increase beyond a transition temperature (T_t) and a final plateau at high temperatures. As MC concentration increases, the transition temperature from which *G'* starts to level off shifts towards lower values (from 55°C at 0.1% w/w, to 37°C at 2.0% w/w). Below and above T_t, MC behaves as a predominantly solid-like material over the whole range of temperatures studied (*G'* dominates over *G''* over the range of frequencies measured), and above T_t, both moduli increase and are still independent of frequency (data not shown) (Funami et al., 2007; L. Li et al., 2001; Lin Li, 2002); the transition temperature thereby corresponds to a weak-to-strong gel transition. The increase in MC concentration also induces a relatively weak change in MC elastic properties (*G'*) at low temperatures, and a much more significant one in the high temperature region, in agreement with previous studies (Nasatto et al., 2015a).

The gelation of MC – whose chains are arranged as 'bundles' at room temperature (or packed 'strands' held together by packing of unsubstituted regions and the hydrophobically-driven aggregation of methyl groups in regions of denser substitution) – has been postulated to follow two steps (Haque & Morris, 1993; Sarkar, 1995; Desbrières, Hirrien, & Rinaudo, 1998; Hirrien, Chevillard, Desbrières, Axelos, & Rinaudo, 1998; Kobayashi, Huang, & Lodge, 1999; L. Li et al., 2001, 2002; Lin Li, 2002; Lin Li, Wang, & Xu, 2003; Funami et al., 2007; Torcello-Gómez & Foster, 2014; Torcello-Gómez et al., 2015; Nasatto et al., 2015a; Isa Ziembowicz et al., 2019): upon heating, MC strands separate, allowing intermolecular associations to form between MC hydrophobic (methyl) groups, therefore inducing the formation of a strong, physical gel network; at low temperatures, these hydrophobic polymer-polymer interactions take place to a much lower extent because of water molecules surrounding MC methyl moieties (*via* hydrogen bonds), thus resulting in the swelling of 'bundles' and the formation of a softer, weaker gel. The effect of MC concentration on its rheological properties is therefore

attributed to the increase in the number of methyl groups in solution, resulting in a larger number of hydrophobic interactions from lower temperatures.

Effect of BS on MC viscoelastic behaviour. The impact of the two BS on MC rheological properties was assessed by following the dynamic moduli (*G'*, *G"*) of a 1.0% w/w MC solution over a range of temperatures and frequencies (Figure 3). The evolution of the transition temperature (T_t, from which the increase in *G'* becomes steeper) and of both dynamic moduli (*G'*, *G"*) are shown as a function of BS concentration in Figures 4A and 4B, respectively.

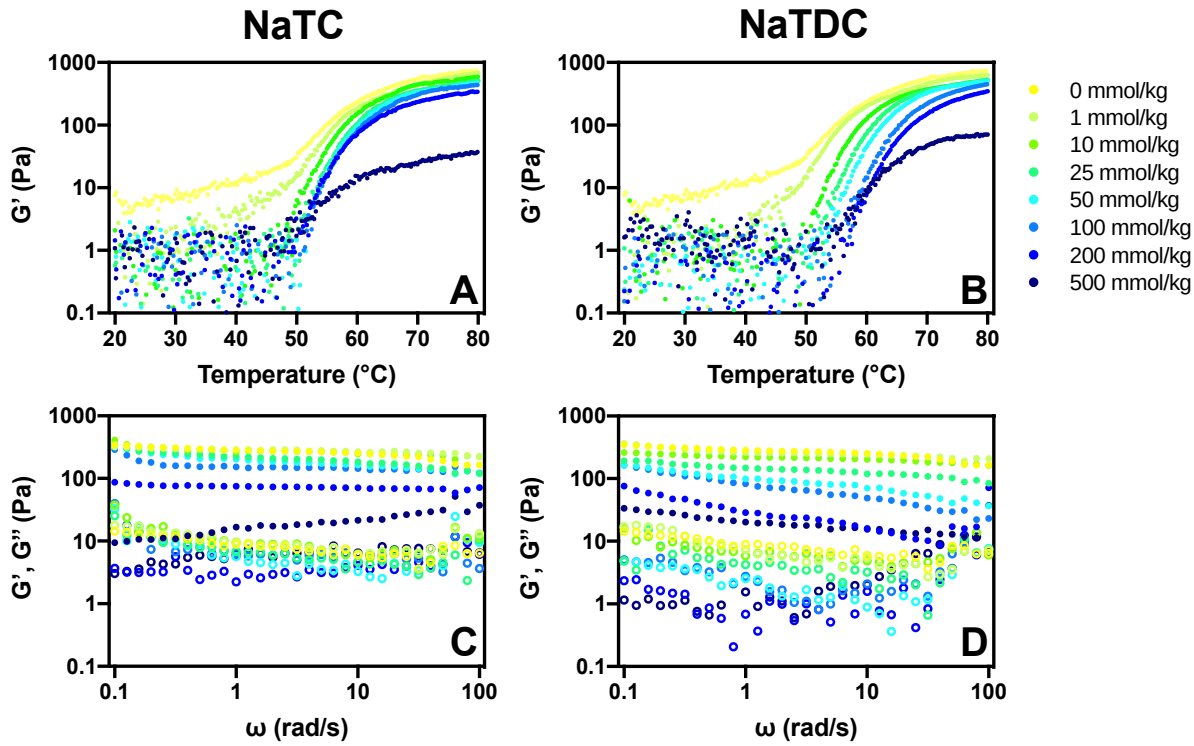

Figure 3: (A, B) Temperature-dependent evolution of the storage modulus (*G'*) obtained from dynamic temperature sweeps, and (C, D) angular frequency-dependent evolution of the dynamic moduli: (●) *G'*, the storage modulus, (○) *G"*, the loss modulus, obtained from dynamic frequency sweeps performed at a constant temperature of 60°C, on a 1.0% w/w MC aqueous solution containing increasing amounts (1, 10, 25, 50, 100, 200, 500 mmol/kg) of BS: (A, C) NaTC, (B, D) NaTDC. The curves obtained in the absence of BS are also shown for comparison.

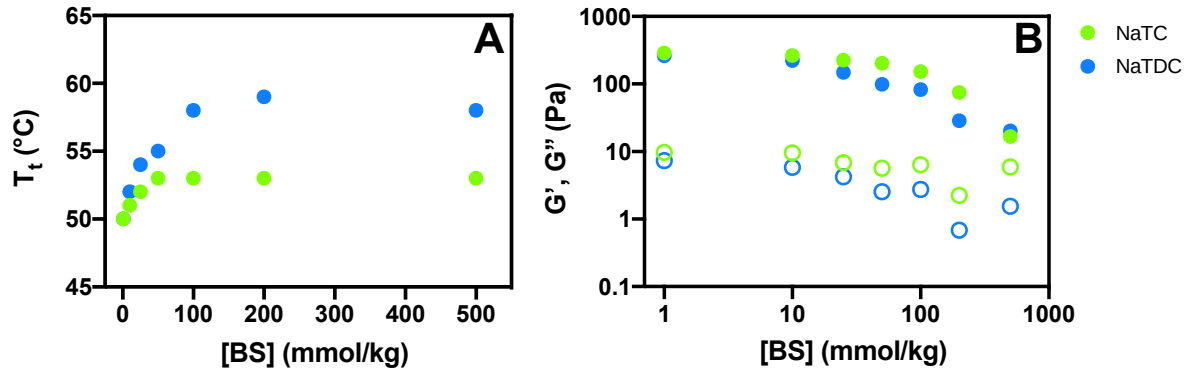

Figure 4: Evolution of MC transition temperature (T_t) (A) and dynamic moduli: (●) *G'*, the storage modulus, (○) *G''*, the loss modulus, obtained at an angular frequency of 1 rad/s (B), as a function of the concentration in BS: NaTC, NaTDC. The transition temperature (T_t) is the temperature from which *G'* starts changing. These data are extracted from, respectively, (A) dynamic temperature sweeps performed over a temperature range of 20 - 80°C (Figures 3, A, B), and (B) dynamic frequency sweeps performed over an angular frequency range of 0.1 - 100 rad/s, at a constant temperature of 60°C (Figures 3, C, D).

In the presence of BS, the dynamic temperature sweeps of MC solutions show a similar profile as the pure MC solution, namely, a moderate increase in *G'* followed by a sharp rise (Figures 3, A, B). However, BS have a significant impact on MC rheological properties, leading to a notable, and gradual increase in the transition temperature from around 50°C, in the absence of BS, to 53°C with 500 mmol/kg NaTC and 58°C with 500 mmol/kg NaTDC (Figure 4A). In addition, both BS (from the lowest concentration studied of 1 mmol/kg) induce a drop in MC viscoelasticity (*G'*) at all temperatures studied, most visibly at high temperatures (Figures 3, A, B). At physiological temperature (37°C), a decrease from G' = 10 Pa in the absence of BS, to G' = 5 and 2 Pa in the presence of 1 mmol/kg of, respectively, NaTC and NaTDC, is observed. Dynamic frequency sweeps performed at 60°C, where MC forms a strong gel and changes caused by BS are most visible (Figures 3, C, D), reveal a 10-fold decrease in *G'*, from ca. 280 Pa in the absence of BS, to ca. 20 Pa with the highest concentration of BS studied, at a frequency of 1 rad/s (Figure 4B). In addition, *G'* shows an increasing dependence on frequency with the addition of BS, more notably so with NaTDC. Overall therefore, the presence of the BS converts MC gel into a less solid-like material. Comparing the two BS, it is clear that NaTDC has a much stronger impact; for instance, only 10 mmol/kg of NaTDC are needed to significantly reduce the value of the storage modulus (*G'*) (Figures 3D and 4B), while 25 mmol/kg of NaTC are required to induce the same effect (Figures 3C and 4B). Similar observations have been reported elsewhere (Torcello-Gómez et al., 2015).

Overall, over the whole temperature range studied, MC behaves as a gel whose strength increases with temperature. The addition of BS induces a transition to a softer material (lower elastic modulus (*G'*)), both above and below MC transition temperature (T_t); in addition, this transition occurs at lower concentrations of NaTDC, compared to NaTC.

3.2 BS interfacial properties in the presence of MC

MC adsorption dynamics at the air/water interface. MC behaviour at the bare air/water interface was studied using both a Langmuir trough and ellipsometer, by monitoring the time-dependent evolution of the surface pressure (π) and phase shift ($\Delta\Delta$), respectively, upon injection into the water subphase of either successive quantities of MC (0.5×10^{-1}, 0.25 and 0.5‰ w/w (Figure S2); 0.5×10^{-2}, 0.25×10^{-1} and 0.5×10^{-1}‰ w/w (Figure S3)), or fixed amounts over a longer period of time (0.5×10^{-3}, 0.5×10^{-2}, 0.5×10^{-1} or 0.5‰ w/w) (Figure S4).

Upon addition of 0.5×10^{-1}‰ w/w MC into the aqueous subphase, the surface pressure increases until reaching a near-plateau at π = 19 ± 1 mN/m, which stays relatively constant with following injections (π = 19 ± 1 mN/m at 0.25‰ w/w, and π = 18 ± 3 mN/m at 0.5‰ w/w) (Figure S2A). With the same injection sequence, the ellipsometry phase shift, which is measured at the same time as the surface pressure and relates to the amount of material adsorbed at the interface (Motschmann & Teppner, 2001), exhibits the same trend as the surface pressure (Figure S2B): it reaches a value of $\Delta\Delta$ = 0.033°, which then slightly increases to $\Delta\Delta$ = 0.035° at 0.25‰ w/w and $\Delta\Delta$ = 0.036 at 0.5‰ w/w. Both measurements thus show that MC adsorbs at the air/water interface up to a saturation point, independently of its concentration in the bulk. The two experiments differ, nevertheless, by the presence of peaks of surface pressure visible straight after MC injection, not detected in the phase shifts, which could be explained by an initial strong adsorption, followed by a relaxation process as the polymer rearranges at the air/water interface, changing conformation (Graham & Phillips, 1979). These transient surface pressure peaks were also observed in a previous study with BS injected under the air/water interface (Pabois et al., 2019). The trends in surface pressure (Figure S3A) and phase shift (Figure S3B) are reproduced with lower amounts of MC (0.5×10^{-2}, 0.25×10^{-1}, and 0.5×10^{-1}‰ w/w) injected into water.

In order to study the kinetics of adsorption of MC molecules at the air/water interface, surface pressure measurements were performed over longer periods of time (Figure S4). Results show that, above 0.5×10^{-2}‰ w/w, the same equilibrium surface pressure (π = 17 ± 1 mN/m) is

always reached, irrespective of MC concentration, whereas a much lower value is obtained at the lowest concentration studied of 0.5×10^{-3}‰ w/w ($\pi = 10 \pm 0.4$ mN/m). Arboleya and Wilde (Arboleya & Wilde, 2005) also observed a saturation point from a similar MC concentration (i.e., 1×10^{-2}‰ w/w), and obtained comparable interfacial tension values. Furthermore, as MC concentration decreases, the surface pressure rises at a slower rate: a change in surface pressure is immediately observed after injection of both 0.5×10^{-1} and 0.5‰ w/w, while a lag period of about 3 and 40 min is seen with solutions containing 0.5×10^{-2} and 0.5×10^{-3}‰ w/w MC, respectively. The amount injected into the aqueous subphase thus affects MC adsorption rate and extent, such that the lower the concentration, the slower the adsorption process and the lower the quantity of material adsorbed, therefore indicating a diffusion-controlled adsorption mechanism, as already observed elsewhere with hydroxypropyl MC (Avranas & Tasopoulos, 2000; Camino, Pérez, Sanchez, Rodriguez Patino, & Pilosof, 2009; Pérez, Sánchez, Pilosof, & Rodríguez Patino, 2008; Wollenweber, Makievski, Miller, & Daniels, 2000). In the literature, MC adsorption has been suggested to occur in three stages: MC first slowly diffuses from the bulk phase to the sub-surface region and then adsorbs at the air/water interface, while undergoing conformational changes (Arboleya & Wilde, 2005).
All these results are consistent with data reported elsewhere (Nasatto et al., 2014; Pizones Ruiz-Henestrosa et al., 2017).

BS interaction with a MC layer at the air/water interface. The interfacial behaviour of the two selected BS (NaTC and NaTDC) in the presence of a MC film at the air/water interface was then evaluated, by injecting BS below the polysaccharide layer. Measurements were carried out either by adding increasing amounts of BS every hour (2, 4, 6, 8 and 10 mM) (Figures 5 and S5) or by injecting fixed concentrations and measuring over longer times (1, 5 or 10 mM) (Figures 6 and S6). These BS concentrations were selected to be below, around, and above their critical micelle concentration (CMC), which is 4 – 7 mM for NaTC (gradual micellisation process) and 2 mM for NaTDC in ultrapure water (data not shown) (Matsuoka, Maeda, & Moroi, 2003). Prior to BS injection, a saturated film of MC at the interface was formed by injecting it into the water subphase, at either 0.5‰ w/w (Figures 5, 6 and S6) or $0.5.10^{-2}$‰ w/w (Figure S5).

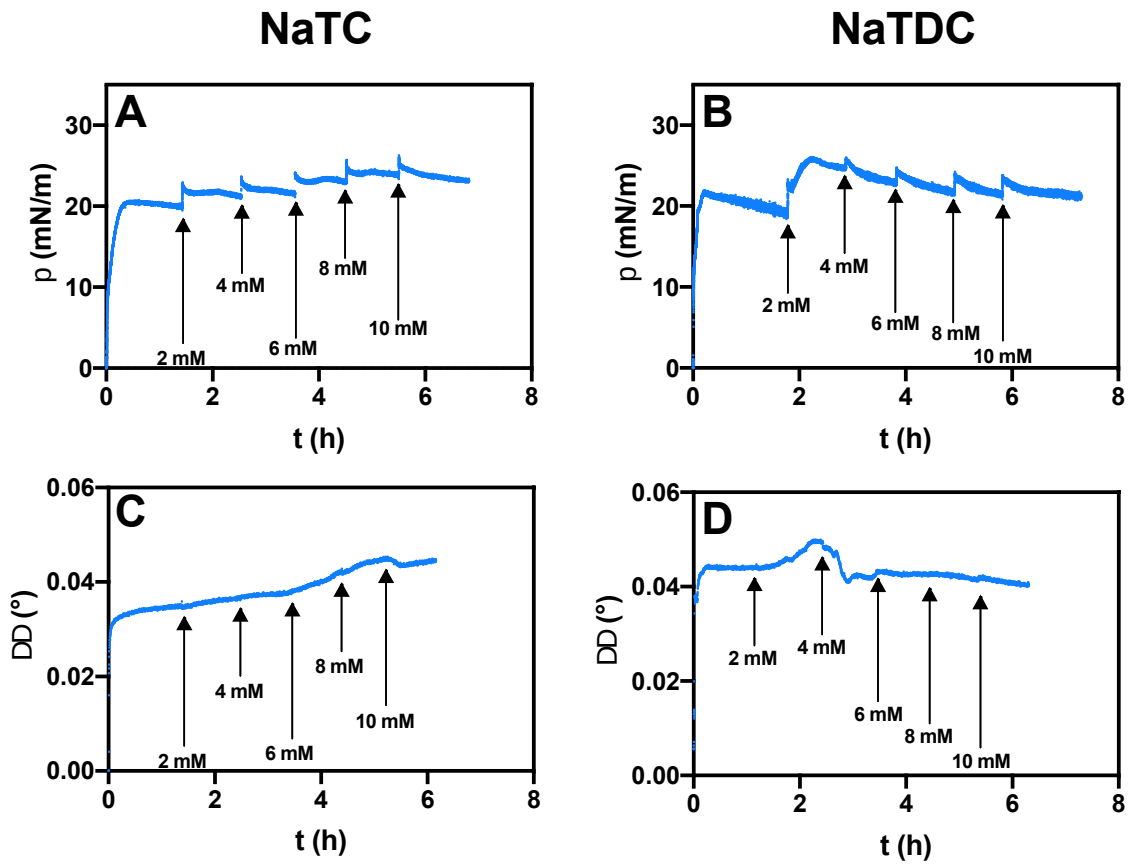

Figure 5: Time-dependent evolution of (A, B) the surface pressure (π) measured in a Langmuir trough, and (C, D) phase shift ($\Delta\Delta(t) = \Delta(t) - \Delta_0$) measured by ellipsometry, upon successive injections of either (A, C) NaTC or (B, D) NaTDC into the aqueous subphase (at 23 ± 2°C). The first increase in surface pressure corresponds to the adsorption of MC at the air/water interface, which was added into water at a concentration of 0.5‰ w/w (π_{MC} = 21 ± 1 mN/m, $\Delta\Delta_{MC}$ = 0.039 ± 0.005°). Each addition of BS is shown by an arrow, together with the corresponding BS concentration achieved in the subphase. Each experiment was reproduced twice, and a representative measurement was selected for each experiment.

The evolution of the surface pressure is quite different for the two BS (Figures 5, A, B): while the successive injections of NaTC lead to a continuous increase in surface pressure (up to π = 23 ± 0.5 mN/m at 10 mM) (Figure 5A), with NaTDC, a steep rise to π = 25 ± 1 mN/m (at 2 mM), followed by a gradual drop to π = 22 ± 1 mN/m (at 10 mM), is observed (Figure 5B). These trends are also obtained with a lower amount of MC at the air/water interface (Figure S5). The ellipsometry phase shift obtained in parallel follows the same trends (Figures 5, C, D): with NaTC, it gradually increases up to ΔΔ = 0.045 ± 0.003° upon successive additions of BS into the subphase (Figure 5C); instead, the injection of 2 mM NaTDC into the water induces a sharp increase to ΔΔ = 0.047 ± 0.003°, followed by a decrease to ΔΔ = 0.042 ± 0.001° from 4 mM (Figure 5D). As observed with successive injections of MC, temporary surface pressure peaks are also present after each addition of BS; here again, these peaks could be attributed to MC

film compression and subsequent relaxation, induced by BS adsorption (Graham & Phillips, 1979).

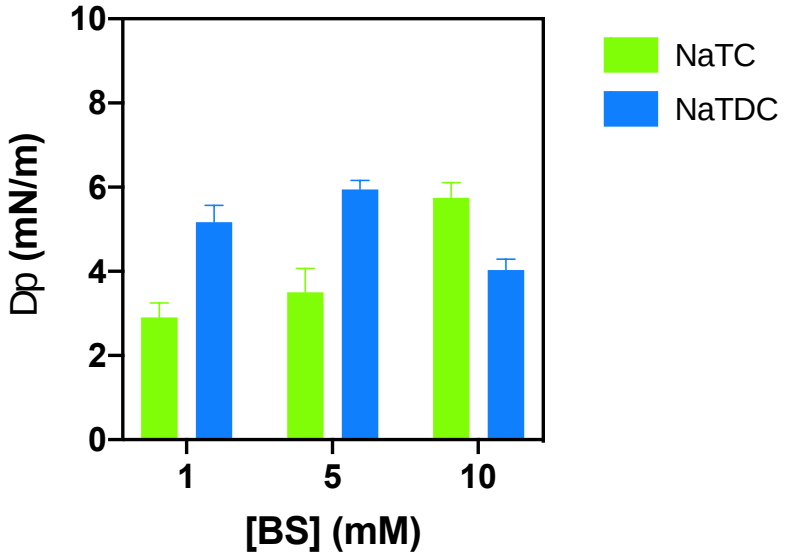

Figure 6: Evolution of the surface pressure ($\Delta\pi = \pi_{Equilibrium} - \pi_{MC}$) as a function of BS concentration, measured in a Langmuir trough, upon injection of fixed concentrations (1, 5, 10 mM) of BS (NaTC, NaTDC) into the aqueous subphase (at 23 ± 2°C). 0.5‰ w/w MC were injected into water to form a layer at the air/water interface, at π_{MC} = 21 ± 1 mN/m. These data were extracted from individual BS injections measurements (Figure S6). Each experiment was reproduced at least twice, and the average measurement was selected for each BS at each concentration.

Upon injection of fixed BS concentrations, the surface pressure increases sharply over time until reaching a plateau value, independently of the BS type and concentration (Figure S6). The surface pressure values achieved at equilibrium are summarised in Figure 6, showing $\Delta\pi = \pi_{Equilibrium} - \pi_{MC}$, where π_{MC} is the initial MC layer surface pressure (π_{MC} = 21 ± 1 mN/m). The surface pressure changes induced by the two BS are relatively small, in agreement with previous studies performed on the interaction of a hydroxypropyl MC layer with bile extract (Pizones Ruiz-Henestrosa et al., 2017). At 1 and 5 mM, NaTDC induces a higher increase in surface pressure ($\Delta\pi$ = 5 ± 0.4 mN/m at 1 mM, and $\Delta\pi$ = 6 ± 0.2 mN/m at 5 mM), compared to NaTC ($\Delta\pi$ = 3 ± 0.3 mN/m at 1 mM, and $\Delta\pi$ = 4 ± 1 mN/m at 5 mM); at high BS concentration (10 mM), the opposite trend is observed ($\Delta\pi$ = 6 ± 0.4 mN/m for NaTC, and $\Delta\pi$ = 4 ± 0.3 mN/m for NaTDC).

3.3 Effect of BS structure and concentration on the duodenal digestion of an MC-stabilised emulsion

A range of *in vitro* duodenal lipolysis studies was carried out on a sunflower oil emulsion stabilised by MC. Before reaching the small intestine, ingested fat droplets pass through simulated oral and gastric digestion, where their physicochemical and structural properties are significantly affected; however, because our main aim is to understand BS roles during lipolysis, the work performed here focuses on the duodenum part of the lipolysis process, where BS are acting.

Evolution of emulsion droplets microstructure. The structure of the pure MC-stabilised emulsion droplets was first characterised using both optical and confocal microscopy (Figure S7). Optical microscopy demonstrates that emulsion droplets are uniformly dispersed with a size ranging between 2 and 5 µm, and with a small number of larger droplets around 10 µm (Figure S7A). Confocal microscopy highlights the presence of a MC network (stained in blue with calcofluor) in the bulk and at the interface of emulsion droplets (stained in red with Nile red) (Figure S7B).

In vitro lipolysis studies were performed on the emulsion by adding the digestive medium and monitoring the structural changes of the emulsion droplets by microscopy (Figures 7, S8 and S9). Using brightfield optical microscopy, the influence of both BS type and concentration on the structure of MC-stabilised emulsion droplets was assessed in control assays (no enzyme), as well as the effect of enzymes (lipolysis assays) (Figure 7). In the absence of enzymes (blank assays), the emulsion droplets microstructure is affected by the digestive fluid, as revealed by the occurrence of droplets flocculation, and some – limited – coalescence, which is more visible with NaTDC, and particularly evident for both BS at high concentration (10 mM). Upon the addition of enzymes (lipolysis assays), flocculation occurs to a higher extent, and droplet coalescence (size increase) is observed in all samples, to a larger extent, again, with NaTDC. To further elucidate the mechanism of digestion of an MC-stabilised emulsion, the influence of the different components of the digestive fluid (NaCl, $CaCl_2$ and BS) on droplet stability was also evaluated (Figures S8 and S9). Brightfield optical micrographs show that extensive flocculation occurs when both BS and salts are present, which suggests that the association of BS with the different salts (NaCl, $CaCl_2$) is responsible for the droplet aggregation observed in Figure 7.

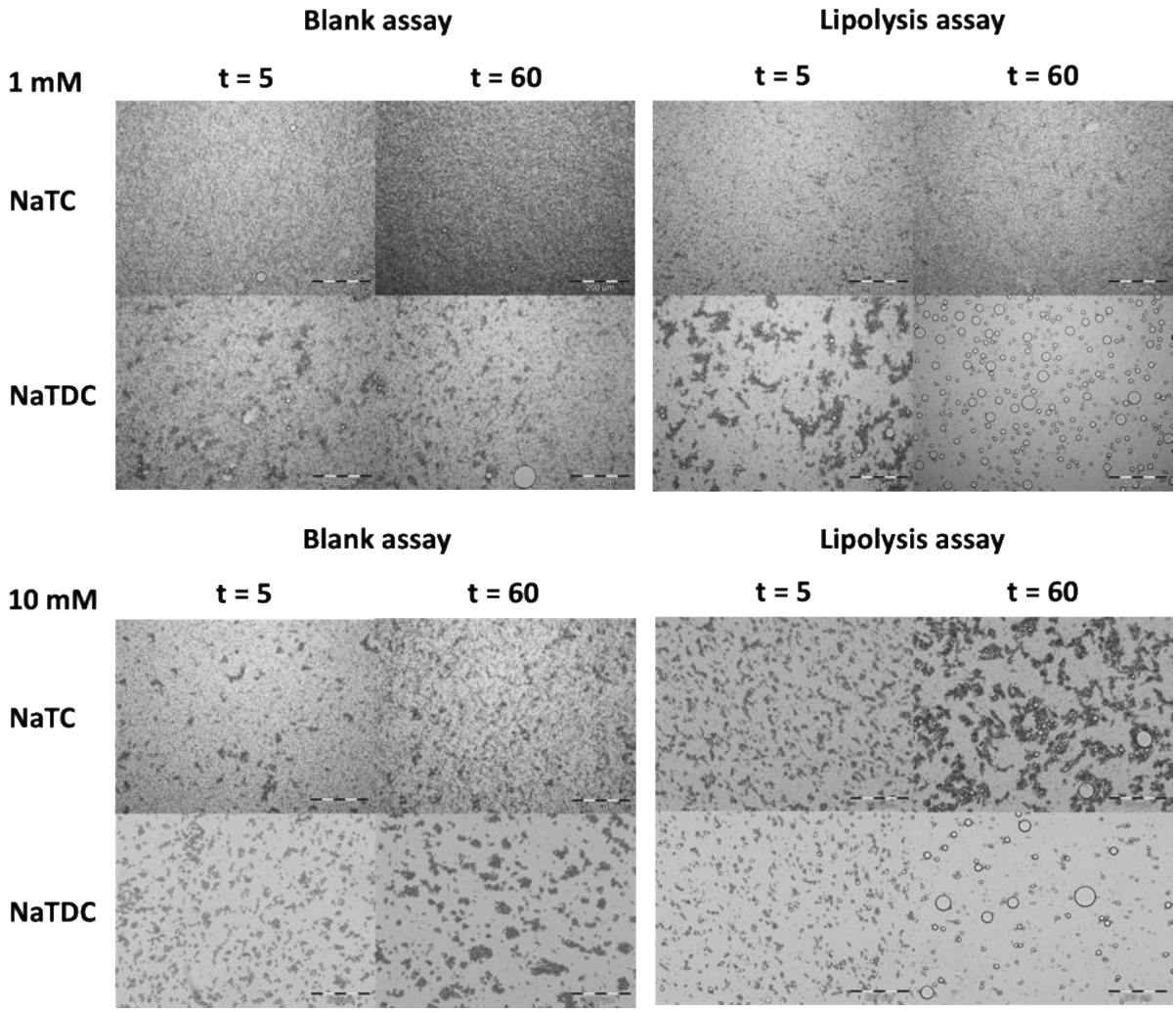

Figure 7: Time-dependent evolution of the microstructure of MC-stabilised emulsion droplets in the presence of BS: NaTC, NaTDC, used at 1 and 10 mM, under duodenal digestion conditions (at 37°C). MC-stabilised emulsion was made up of 0.5% MC and 15% sunflower oil. Both blank (without enzymes) and lipolysis (with enzymes) assays were performed to assess, respectively, the effect of BS type and concentration on the droplets stability, and of enzymes on the droplets microstructure. Microscopy observations were made at t = 5 and 60 minutes. The scale bar is 200 µm.

This *in vitro* lipolysis study was complemented with micro-structural assessment of the emulsion droplets with confocal microscopy, to determine the localisation of MC throughout the emulsion and its evolution during lipid digestion (Figures 8 and 9). Based on our pH-stat results (see the following section), 50 mM BS was used here, as it shows the higher extent of FFA release. The images obtained suggest that the addition of digestive fluid not only breaks down the network of MC, but also displaces it from the lipid/water interface (Figure 8); interestingly, MC bulk network is disrupted to a higher extent in the presence of NaTDC, compared to NaTC. Additionally, the lipid droplets become non-spherical with "rough" surfaces, compared to the initial emulsion (Figures 8 and 9). This demonstrates coalescence

and may be an indication of fats being digested by enzymes; in particular, small oil droplets were seen to flocculate or coalesce onto the surface of larger droplets (Figure 9A) and areas with an undefined oil/water interface suggest the presence of digestion products (Figure 9B).

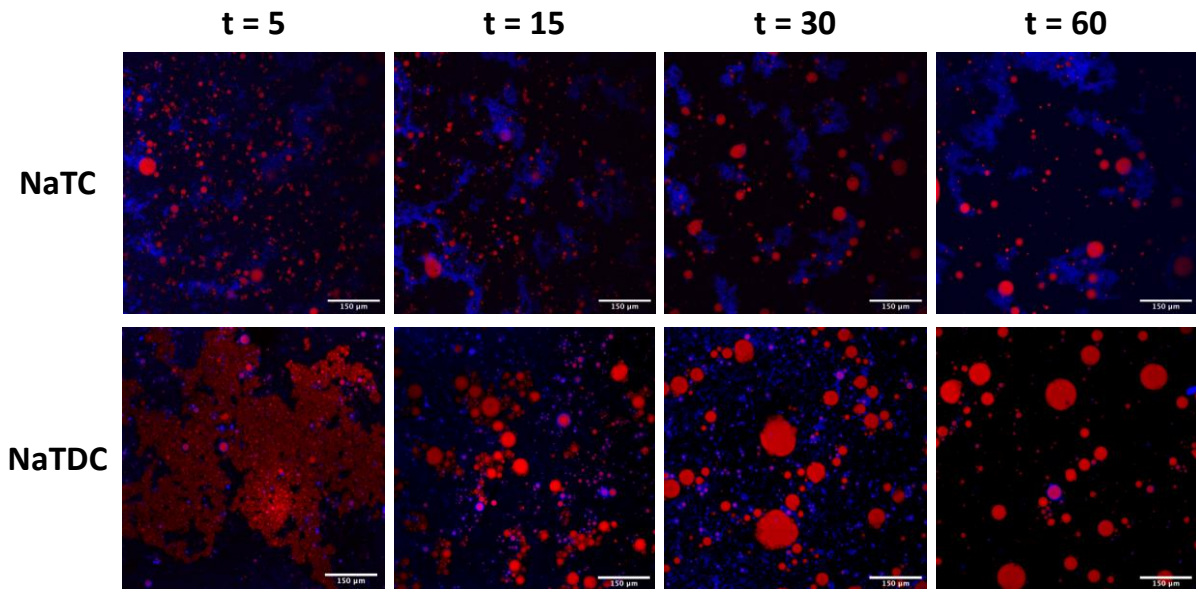

Figure 8: Time-dependent evolution of the microstructure of MC-stabilised emulsion droplets in the presence of 50 mM BS: NaTC, NaTDC, under duodenal digestion conditions (at 37°C). MC-stabilised emulsion was made up of 0.5% MC and 15% sunflower oil. The lipid droplets are stained in red (with Nile red), while MC is stained in blue (with calcofluor). Microscopy observations were made at t = 5, 15, 30 and 60 minutes, to compare the structural changes occurring during digestion; at each time point, orlistat was used to inhibit lipolysis. The scale bar is 150 µm.

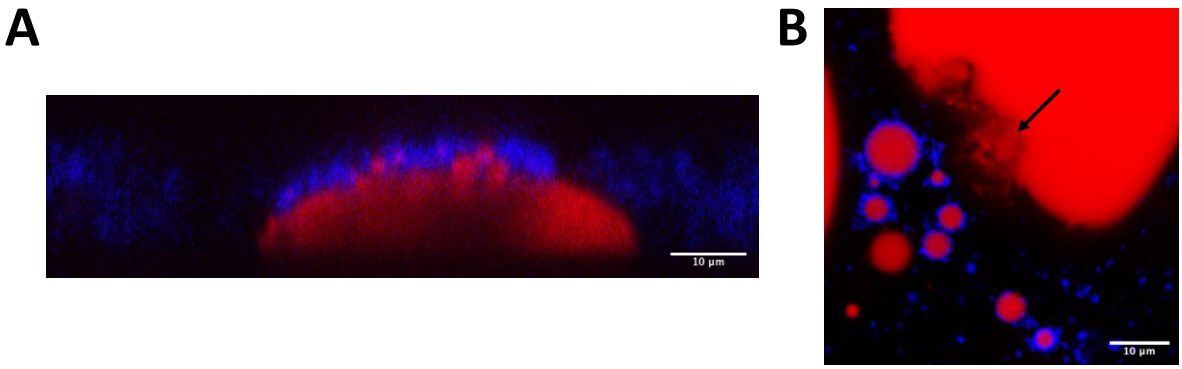

Figure 9: (A) Cross-section confocal image of MC-stabilised emulsion droplets in the presence of 50 mM NaTC, under duodenal digestion conditions (at 37°C). The microscopy observation was made at t = 15 minutes. (B) MC-stabilised emulsion droplets in the presence of 50 mM NaTDC, under duodenal digestion conditions (at 37°C). Insoluble lipolysis products seem to be presumably present at the fat droplet interface (see the arrow). MC-stabilised emulsion was made up of 0.5% MC and 15% sunflower oil. The lipid droplets are stained in red (with Nile red), while MC is stained in blue (with calcofluor). The scale bar is 10 µm.

Quantification of FFA release from the MC-stabilised emulsion. The ability of NaTC and NaTDC to promote or inhibit the duodenal digestion of an MC-stabilised emulsion was compared by monitoring the release of FFA (*%FFA*) over time with the pH-stat method (Y. Li, Hu, & McClements, 2011) (Figure 10). The effect of BS concentration on the rate of lipolysis and its extent was also evaluated using the two BS at both 10 and 50 mM.

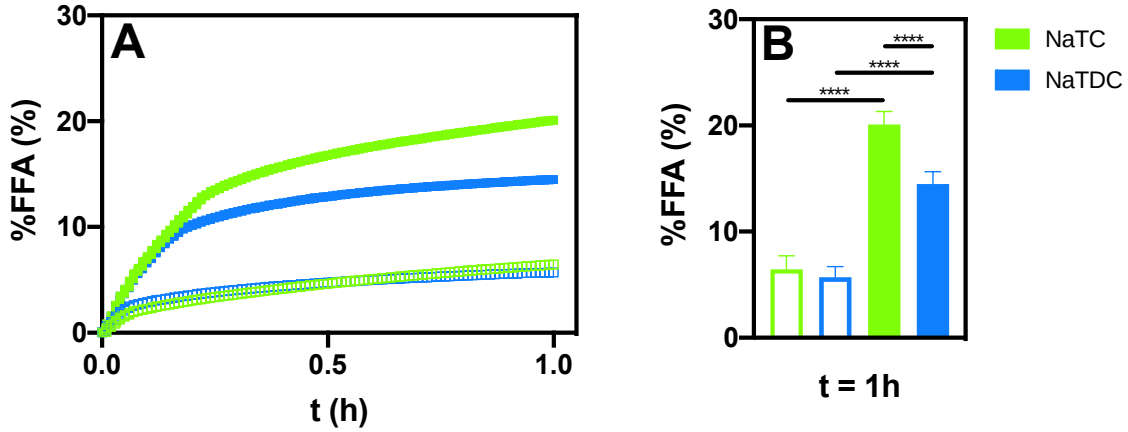

Figure 10: (A) Proportion of FFA released (*%FFA*) over time from an MC-stabilised emulsion, using two different BS: NaTC, NaTDC, at two different concentrations: (□) 10 and (■) 50 mM, under duodenal digestion conditions (at 37°C). (B) Proportion of FFA released (*%FFA*) after 1 hour of digestion of an MC-stabilised emulsion, using the two BS, at 10 and 50 mM, under duodenal digestion conditions (at 37°C). Statistical significance was determined using the two-way ANOVA, followed by the Tukey post-test (** indicates P < 0.0001, i.e., differences are extremely significant). MC-stabilised emulsion was made up of 0.5% MC and 15% sunflower oil.**

Independently of the BS type and concentration, the proportion of FFA generated during lipolysis increases steeply after the addition of enzymes (Figure 10A); this rapid initial rate of lipolysis, already observed elsewhere (Bellesi, Martinez, Pizones Ruiz-Henestrosa, & Pilosof, 2016; McClements & Li, 2010a), can be attributed to the immediate adsorption of lipase/co-lipase onto fat droplets surfaces, which then triggers TAG break-down and thus lipid digestion. After a certain time (t = 0.07 h with both BS at 10 mM, t = 0.18 h with 50 mM NaTDC and t = 0.24 h with 50 mM NaTC), the release of FFA starts slowing down, until it reaches a near-plateau. This decrease in the rate of lipolysis can be explained by the accumulation of lipolysis products at the oil/water interface during the process of fat digestion (Patton & Carey, 1979; P. Reis, Holmberg, Watzke, Leser, & Miller, 2009; P. Reis et al., 2008; P. M. Reis et al., 2008), which then leads to the inhibition of enzymes binding to the substrate, as previously demonstrated (Bellesi et al., 2016; Borel et al., 1994). Increasing BS concentration from 10 to 50 mM leads to a significant increase in the percentage of FFA produced, for both BS (P_{NaTC} <

542 0.0001 and $P_{NaTDC} < 0.0001$) (Figure 10B): more specifically, a 14% and 9% increase is obtained
543 with, respectively, NaTC and NaTDC. This can be attributed to the larger amount of BS
544 micelles, which can solubilise a larger amount of FFA released, thereby preventing droplets
545 surface saturation by these products (Wilde & Chu, 2011). While no significant differences are
546 observed between the two BS at the lowest concentration (10 mM) ($\%FFA_{t = 1h} = 6 \pm 1$ % for
547 both NaTC and NaTDC; $P_{10\ mM} = 0.4$), a significant difference is seen at high concentration (50
548 mM), with NaTC inducing a higher extent of lipolysis ($\%FFA_{t = 1h} = 20 \pm 1$ % and 14 ± 1 % for,
549 respectively, NaTC and NaTDC; $P_{50\ mM} < 0.0001$).

4. Discussion

The objective of this study was to investigate the interactions of MC with BS, in particular the ability of MC to inhibit BS activity, and thus to shed light on the mechanism of lipid digestion regulation by MC – a dietary fibre with a proven potential to lower cholesterol levels (Agostoni et al., 2010). Bulk (rheology) and interfacial (surface pressure measurements and ellipsometry) studies were carried out to characterise the interactions between these two components in the bulk and at the interface, while *in vitro* lipolysis (microscopy, pH-stat) experiments were performed to link these interactions to the lipid digestion of an MC-stabilised emulsion. The two BS, which differ by the presence (NaTC) or absence (NaTDC) of a hydroxyl group on their steroid skeleton (Figure 2) and constitute 20% of human bile (Staggers, Hernell, Stafford, & Carey, 1990), were chosen for this study, as they have been reported to exhibit different interfacial behaviours, hypothesised to explain the contrasting roles they play during the process of lipolysis (Pabois et al., 2019; Parker et al., 2014).

4.1 Interaction between MC and BS in the bulk and at the interface

The impact of BS on MC rheological properties was investigated to explore the interaction of BS with MC in the bulk, where MC is present in excess. Increasing the amount of BS in solution led to a notable shift in the transition temperature (T_t) to higher values, as well as a gradual drop in viscoelastic properties, which were more substantial with NaTDC (Figures 3 and 4). In particular, MC – which presents predominantly solid-like properties in the absence of BS – turned into a softer gel above a threshold concentration of BS (25 mmol/kg for NaTC *vs*. 10 mmol/kg for NaTDC, at 60°C) (Figures 3, C, D and 4B). MC gelation occurs *via* the association of the hydrophobic (methyl) moieties (Haque & Morris, 1993; Sarkar, 1995; Desbrières, Hirrien, & Rinaudo, 1998; Hirrien, Chevillard, Desbrières, Axelos, & Rinaudo, 1998; Kobayashi, Huang, & Lodge, 1999; L. Li et al., 2001, 2002; Lin Li, 2002; Lin Li, Wang, & Xu, 2003; Funami et al., 2007; Torcello-Gómez & Foster, 2014; Torcello-Gómez et al., 2015; Nasatto et al., 2015a; Isa Ziembowicz et al., 2019). The presence of BS and its association with MC may thus prevent hydrophobic groups from assembling with each other, thus weakening the gels or hindering gelation altogether. The stronger effect observed with NaTDC may be attributed to its higher hydrophobicity (Armstrong & Carey, 1982), which may result in a more efficient connection between BS and MC hydrophobic regions (Torcello-Gómez et al., 2015). Overall,

these rheological measurements reveal the presence of strong interactions between BS and the dietary fibre, which have a substantial impact on MC viscosity; the presence (NaTC) or absence (NaTDC) of a hydroxyl group on BS steroid backbone impacts this behaviour considerably.

The interfacial properties of BS in the presence of a MC layer formed at the air/water interface were then studied to determine the interactions occurring when a BS molecule approaches a fat droplet stabilised by MC. Studies with a Langmuir trough set-up (Figures 5, A, B, S5, 6 and S6) combined to ellipsometry (Figures 5, C, D) demonstrate that the two BS behave quite differently when injected beneath an almost-saturated MC film: NaTC was shown to gradually adsorb at the interface with increasing concentration, whereas NaTDC first adsorbed at low concentrations (up to 2 – 3 mM) and then desorbed above 4 – 5 mM. This contrasting interfacial behaviour correlates with their micellisation behaviour, which occurs over 4 – 7 mM for NaTC and at 2 mM for NaTDC. Similar differences have been observed when BS were injected below a phospholipid monolayer (Pabois et al., 2019). Nevertheless, BS were found to adsorb and/or desorb to a much lower extent in the presence of a MC film, compared to the phospholipid monolayer (surface pressures changes as high as 30 mN/m were monitored in the presence of the lipid film, whereas an increase of up to 10 mN/m was observed with the MC layer). This may in part be explained by the likely presence of MC excess in the bulk, which could interact with BS and therefore limit their adsorption at the interface.

4.2 Impact of BS/MC interactions on fat digestion

Next, we performed *in vitro* lipolysis studies by following the evolution of the structure of an MC-stabilised emulsion with optical and confocal microscopy, to compare the effect of the two BS on the droplets (Figures S7A and 7) and shed light on the behaviour of MC during emulsion digestion (Figures S7B, 8 and 9). The characterisation of the MC-stabilised emulsion by confocal microscopy clearly demonstrates that fat droplets are entrapped in a network of MC present in excess in the bulk, which may be responsible for the stabilisation of the emulsion against droplets flocculation or coalescence (Figure S7B). Optical microscopy images (Figure 7) demonstrate that, even in the absence of digestive enzymes, the presence of both BS destabilises the emulsion, inducing some flocculation; upon the addition of lipases, droplets destabilisation (namely, flocculation and coalescence) was found to occur to a large

610 extent, and more markedly with NaTDC, compared to NaTC. Confocal microscopy images
611 (Figure 8) suggest that flocculation and coalescence observed during lipolysis are due to the
612 MC network being broken down and removed from the lipid/water interface. The better
613 ability of NaTDC to induce coalescence could therefore be explained by its higher capacity to
614 disturb MC bulk network (as observed by confocal microscopy observations), which, in turn,
615 could be attributed to its stronger interactions with MC (as seen from rheology
616 measurements) and higher propensity to desorb from the interface at lower concentrations
617 (as detected by interfacial measurements). While the displacement of MC from the interface
618 by BS may facilitate the access of BS and enzymes to the lipid droplets surface, the network of
619 MC remaining in the bulk may also trap BS (*via* hydrophobic interactions) and thus prevent
620 them from removing insoluble lipolysis products, which could explain how MC hinders lipase
621 activity. Emulsion droplets coalescence (and thus the decrease in droplets surface area), which
622 occurs under duodenal digestion conditions, could also explain the slowing down of lipolysis.

623 The capacity of the two BS to promote or inhibit MC-stabilised emulsion digestion was
624 then explored with the pH-stat method; results revealed that NaTC favoured FFA release to a
625 higher extent than NaTDC (at 50 mM) (Figure 10). The lower proportion of FFA release
626 obtained with NaTDC can be explained by its higher efficiency at binding to MC network (as
627 suggested by rheology measurements), which may result in this BS becoming trapped in the
628 bulk and therefore not contributing to the lipolysis process.

5. Conclusion

The demonstrated potential of MC, a dietary fibre, to regulate lipolysis is thought to be due to its ability to reduce BS activity by sequestration; the objective of this work was to compare the interactions of two structurally different BS, NaTC and NaTDC, with MC, and to determine their impact on the digestion of an emulsion stabilised by this polysaccharide. These findings are key to establishing a molecular-level, mechanistic understanding of the ability of MC to lower fat absorption.

Both BS were found to decrease the elasticity of MC gels, and to shift the transition temperature (T_t) to stiffer gels to higher temperatures, to a higher extent with NaTDC. When injected below a MC film at the air/water interface, NaTC remained adsorbed at the interface over a wider concentration range, compared to NaTDC, which desorbed at a lower concentration, correlating with the onset of micellisation in the bulk (between 4 – 7 mM for NaTC and at 2 mM for NaTDC). The small difference in the two BS molecular structure, specifically their bile acid portion, is responsible for their contrasting behaviour, and explains the different results obtained during *in vitro* lipid digestion: (i) NaTDC has a higher propensity to disrupt MC network in the bulk and interfacial layer, and thus induces more extensive emulsion destabilisation (as seen from optical and confocal microscopy); (ii) the release of FFA is lower with NaTDC, which can be linked to its higher capacity to bind MC in the bulk, resulting in BS being unable to access the oil/water interface. Overall, it is clear that BS architectural diversity – whose importance is often neglected – plays a key role in their functionalities during fat digestion.

This work is a first step towards unlocking the mechanism of lipid digestion regulation by MC. Additional structural studies, in particular with techniques such as small-angle neutron scattering and neutron reflectometry, should bring significant knowledge to the area, in particular to examine the structure of MC in the presence of BS and the evolution of the fat droplet interface during digestion; this is the focus of current work. Building upon these results, the next challenge will be to engineer MC-stabilised lipid emulsions with appetite-suppressing or satiety-enhancing properties and evaluate their effect on cholesterol levels.

Acknowledgements

The Institut Laue-Langevin (ILL, Grenoble, France) is acknowledged for the provision of a PhD studentship (OP). The authors acknowledge the Partnership for Soft Condensed Matter (PSCM) for access to sample preparation facilities and the use of the Langmuir trough, ellipsometer and optical microscope. Prof Peter Ellis is thanked for many useful discussions and access to laboratory facilities. OP also thanks Dr Angélique Pabois for her kind help with the statistical analysis of pH-stat data, and Taniya Akhtar for her contribution to the project. PJW and MM-LG gratefully acknowledge the support of the Biotechnology and Biological Sciences Research Council (BBSRC) through the BBSRC Institute Strategic Programme Food Innovation and Health BB/R012512/1 and its constituent project BBS/E/F/000PR10345. Dr Isabelle Grillo, one of our co-authors and OP's PhD co-supervisor, sadly passed away during the writing-up of this manuscript; we dedicate this to her memory.

Declarations of interest

None

References

Agostoni, C., Bresson, J.-L., Fairweather-Tait, S., Flynn, A., Golly, I., Korhonen, H., … Verhagen, H. (2010). Scientific opinion on the substantiation of health claims related to hydroxypropyl methylcellulose (HPMC) and maintenance of normal bowel function (ID 812), reduction of post-prandial glycaemic responses (ID 814), maintenance of normal blood cholesterol c. *EFSA Journal*, *8*(10), 1739. https://doi.org/10.2903/j.efsa.2010.1739

Arboleya, J.-C., & Wilde, P. J. (2005). Competitive adsorption of proteins with methylcellulose and hydroxypropyl methylcellulose. *Food Hydrocolloids*, *19*(3), 485–491. https://doi.org/10.1016/j.foodhyd.2004.10.013

Armstrong, M. J., & Carey, M. C. (1982). The hydrophobic-hydrophilic balance of bile salts. Inverse correlation between reverse-phase high performance liquid chromatographic mobilities and micellar cholesterol-solubilizing capacities. *Journal of Lipid Research*, *23*(1), 70–80. Retrieved from http://www.ncbi.nlm.nih.gov/pubmed/7057113

Avranas, A., & Tasopoulos, V. (2000). Aqueous solutions of sodium deoxycholate and hydroxypropylmethylcellulose: dynamic surface tension measurements. *Journal of Colloid and Interface Science*, *221*(2), 223–229. https://doi.org/10.1006/jcis.1999.6574

Bartley, G. E., Yokoyama, W., Young, S. A., Anderson, W. H. K., Hung, S.-C., Albers, D. R., … Kim, H. (2010). Hypocholesterolemic effects of hydroxypropyl methylcellulose are mediated by altered gene expression in hepatic bile and cholesterol pathways of male hamsters. *The Journal of Nutrition*, *140*(7), 1255–1260. https://doi.org/10.3945/jn.109.118349

Bellesi, F. A., Martinez, M. J., Pizones Ruiz-Henestrosa, V. M., & Pilosof, A. M. R. (2016). Comparative behavior of protein or polysaccharide stabilized emulsion under in vitro gastrointestinal conditions. *Food Hydrocolloids*, *52*, 47–56. https://doi.org/10.1016/j.foodhyd.2015.06.007

Borel, P., Armand, M., Ythier, P., Dutot, G., Melin, C., Senft, M., … Lairon, D. (1994). Hydrolysis of emulsions with different triglycerides and droplet sizes by gastric lipase in vitro. Effect on pancreatic lipase activity. *The Journal of Nutritional Biochemistry*, *5*(3), 124–133. https://doi.org/10.1016/0955-2863(94)90083-3

Borgström, B., Erlanson-Albertsson, C., & Wieloch, T. (1979). Pancreatic colipase: chemistry and physiology. *Journal of Lipid Research*, *20*(7), 805–816. Retrieved from http://www.ncbi.nlm.nih.gov/pubmed/385801

Bourbon Freie, A., Ferrato, F., Carrière, F., & Lowe, M. E. (2006). Val-407 and Ile-408 in the β5'-loop of pancreatic lipase mediate lipase-colipase interactions in the presence of bile salt micelles. *Journal of Biological Chemistry*, *281*(12), 7793–7800. https://doi.org/10.1074/jbc.M512984200

Camino, N. A., Pérez, O. E., Sanchez, C. C., Rodriguez Patino, J. M., & Pilosof, A. M. R. (2009). Hydroxypropylmethylcellulose surface activity at equilibrium and adsorption dynamics at the air–water and oil–water interfaces. *Food Hydrocolloids*, *23*(8), 2359–2368. https://doi.org/10.1016/j.foodhyd.2009.06.013

Carr, T. P., Gallaher, D. D., Yang, C.-H., & Hassel, C. A. (1996). Increased intestinal contents viscosity reduces cholesterol absorption efficiency in hamsters fed hydroxypropyl methylcellulose. *The Journal of Nutrition*, *126*(5), 1463–1469. https://doi.org/10.1093/jn/126.5.1463

Desbrières, J., Hirrien, M., & Rinaudo, M. (1998). A calorimetric study of methylcellulose gelation. *Carbohydrate Polymers*, *37*, 145–152.

Erlanson-Albertsson, C. (1983). The interaction between pancreatic lipase and colipase: a protein-protein interaction regulated by a lipid. *FEBS Letters*, *162*(2), 225–229. https://doi.org/10.1016/0014-5793(83)80760-1

Fiji. (2019). Retrieved July 29, 2019, from https://fiji.sc/

Funami, T., Kataoka, Y., Hiroe, M., Asai, I., Takahashi, R., & Nishinari, K. (2007). Thermal aggregation of methylcellulose with different molecular weights. *Food Hydrocolloids*, *21*(1), 46–58. https://doi.org/10.1016/j.foodhyd.2006.01.008

Graham, D. E., & Phillips, M. C. (1979). Proteins at liquid interfaces. I. Kinetics of adsorption and surface denaturation. *Journal of Colloid and Interface Science*, *70*(3), 403–414. https://doi.org/10.1016/0021-9797(79)90048-1

GraphPad Prism. (2019). Retrieved June 28, 2019, from https://www.graphpad.com/scientific-software/prism/

Grundy, M. M. L., Wilde, P. J., Butterworth, P. J., Gray, R., & Ellis, P. R. (2015). Impact of cell wall encapsulation of almonds on in vitro duodenal lipolysis. *Food Chemistry*, *185*, 405–412. https://doi.org/10.1016/j.foodchem.2015.04.013

Gunness, P., & Gidley, M. J. (2010). Mechanisms underlying the cholesterol-lowering properties of soluble dietary fibre polysaccharides. *Food and Function*, *1*(2), 149–155. https://doi.org/10.1039/c0fo00080a

Haque, A., & Morris, E. R. (1993). Thermogelation of methylcellulose. Part I: molecular structures and processes. *Carbohydrate Polymers*, *22*(3), 161–173. https://doi.org/10.1016/0144-8617(93)90137-S

Hirrien, M., Chevillard, C., Desbrières, J., Axelos, M. A. V, & Rinaudo, M. (1998). Thermogelation of methylcelluloses: new evidence for understanding the gelation mechanism. *Polymer*, *39*(25), 6251–6259. https://doi.org/10.1016/S0032-3861(98)00142-6

Hofmann, A. F., & Mysels, K. J. (1987). Bile salts as biological surfactants. *Colloids and Surfaces*, *30*(1), 145–173. https://doi.org/10.1016/0166-6622(87)80207-X

Isa Ziembowicz, F., de Freitas, D. V., Bender, C. R., dos Santos Salbego, P. R., Piccinin Frizzo, C., Pinto Martins, M. A., … Villetti, M. A. (2019). Effect of mono- and dicationic ionic liquids on the viscosity and thermogelation of methylcellulose in the semi-diluted regime. *Carbohydrate Polymers*, *214*, 174–185. https://doi.org/10.1016/j.carbpol.2019.02.095

Kobayashi, K., Huang, C., & Lodge, T. P. (1999). Thermoreversible gelation of aqueous methylcellulose solutions. *Macromolecules*, *32*(21), 7070–7077. https://doi.org/10.1021/ma990242n

Labourdenne, S., Brass, O., Ivanova, M., Cagna, A., & Verger, R. (1997). Effects of colipase and bile salts on the catalytic activity of human pancreatic lipase. A study using the oil drop tensiometer. *Biochemistry*, *36*(12), 3423–3429. https://doi.org/10.1021/bi961331k

Li, L., Shan, H., Yue, C. Y., Lam, Y. C., Tam, K. C., & Hu, X. (2002). Thermally induced association and dissociation of methylcellulose in aqueous solutions. *Langmuir*, *18*(20), 7291–7298. https://doi.org/10.1021/la020029b

Li, L., Thangamathesvaran, P. M., Yue, C. Y., Tam, K. C., Hu, X., & Lam, Y. C. (2001). Gel network structure of methylcellulose in water. *Langmuir*, *17*(26), 8062–8068. https://doi.org/10.1021/la010917r

Li, Lin. (2002). Thermal gelation of methylcellulose in water: scaling and thermoreversibility. *Macromolecules*, *35*(15), 5990–5998. https://doi.org/10.1021/ma0201781

Li, Lin, Wang, Q., & Xu, Y. (2003). Thermoreversible association and gelation of methylcellulose in aqueous solutions. *Nihon Reoroji Gakkaishi*, *31*(5), 287–296. https://doi.org/10.1678/rheology.31.287

Li, Y., Hu, M., & McClements, D. J. (2011). Factors affecting lipase digestibility of emulsified lipids using an in vitro digestion model: proposal for a standardised pH-stat method. *Food Chemistry*, *126*(2), 498–505. https://doi.org/10.1016/j.foodchem.2010.11.027

Maki, K. C., Carson, M. L., Kerr Anderson, W. H., Geohas, J., Reeves, M. S., Farmer, M. V., … Rains, T. M. (2009). Lipid-altering effects of different formulations of hydroxypropylmethylcellulose. *Journal of Clinical Lipidology*, *3*(3), 159–166. https://doi.org/10.1016/j.jacl.2009.04.053

Maldonado-Valderrama, J., Wilde, P., Macierzanka, A., & Mackie, A. (2011). The role of bile salts in digestion. *Advances in Colloid and Interface Science*, *165*(1), 36–46. https://doi.org/10.1016/j.cis.2010.12.002

Matsuoka, K., Maeda, M., & Moroi, Y. (2003). Micelle formation of sodium glyco- and taurocholates and sodium glyco- and taurodeoxycholates and solubilization of cholesterol into their micelles. *Colloids and Surfaces B: Biointerfaces*, *32*(2), 87–95. https://doi.org/10.1016/S0927-7765(03)00148-6

McClements, D. J., & Li, Y. (2010a). Review of in vitro digestion models for rapid screening of emulsion-based systems. *Food & Function*, *1*, 32–59.

https://doi.org/10.1039/c0fo00111b

McClements, D. J., & Li, Y. (2010b). Structured emulsion-based delivery systems: controlling the digestion and release of lipophilic food components. *Advances in Colloid and Interface Science*, *159*(2), 213–228. https://doi.org/10.1016/j.cis.2010.06.010

Mei, J., Lindqvist, A., Krabisch, L., Rehfeld, J. F., & Erlanson-Albertsson, C. (2006). Appetite suppression through delayed fat digestion. *Physiology & Behavior*, *89*(4), 563–568. https://doi.org/10.1016/j.physbeh.2006.07.020

Motschmann, H., & Teppner, R. (2001). Ellipsometry in interface science. In D. Möbius & R. Miller (Eds.), *Studies in interface science - Novel methods to study interfacial layers* (1st ed., pp. 1–42). Amsterdam: Elsevier Science B. V.

Nasatto, P. L., Pignon, F., Silveira, J. L. M., Duarte, M. E. R., Noseda, M. D., & Rinaudo, M. (2014). Interfacial properties of methylcelluloses: the influence of molar mass. *Polymers*, *6*(12), 2961–2973. https://doi.org/10.3390/polym6122961

Nasatto, P. L., Pignon, F., Silveira, J. L. M., Duarte, M. E. R., Noseda, M. D., & Rinaudo, M. (2015a). Influence of molar mass and concentration on the thermogelation of methylcelluloses. *International Journal of Polymer Analysis and Characterization*, *20*(2), 110–118. https://doi.org/10.1080/1023666X.2015.973155

Nasatto, P. L., Pignon, F., Silveira, J. L. M., Duarte, M. E. R., Noseda, M. D., & Rinaudo, M. (2015b). Methylcellulose, a cellulose derivative with original physical properties and extended applications. *Polymers*, *7*(5), 777–803. https://doi.org/10.3390/polym7050777

Pabois, O., Lorenz, C. D., Harvey, R. D., Grillo, I., Grundy, M. M.-L., Wilde, P. J., … Dreiss, C. A. (2019). Molecular insights into the behaviour of bile salts at interfaces: a key to their role in lipid digestion. *Journal of Colloid and Interface Science*, *556*, 266–277. https://doi.org/10.1016/j.jcis.2019.08.010

Parker, R., Rigby, N. M., Ridout, M. J., Gunning, A. P., & Wilde, P. J. (2014). The adsorption–desorption behaviour and structure function relationships of bile salts. *Soft Matter*, *10*(34), 6457–6466. https://doi.org/10.1039/c4sm01093k

809 Patton, J., & Carey, M. (1979). Watching fat digestion. *Science*, *204*(4389), 145–148.
810 https://doi.org/10.1126/science.432636

811 Pérez, O. E., Sánchez, C. C., Pilosof, A. M. R., & Rodríguez Patino, J. M. (2008). Dynamics of
812 adsorption of hydroxypropyl methylcellulose at the air–water interface. *Food*
813 *Hydrocolloids*, *22*(3), 387–402. https://doi.org/10.1016/j.foodhyd.2006.12.005

814 Pilosof, A. M. R. (2017). Potential impact of interfacial composition of proteins and
815 polysaccharides stabilized emulsions on the modulation of lipolysis. The role of bile salts.
816 *Food Hydrocolloids*, *68*, 178–185. https://doi.org/10.1016/j.foodhyd.2016.08.030

817 Pizones Ruiz-Henestrosa, V. M., Bellesi, F. A., Camino, N. A., & Pilosof, A. M. R. (2017). The
818 impact of HPMC structure in the modulation of in vitro lipolysis: the role of bile salts.
819 *Food Hydrocolloids*, *62*, 251–261. https://doi.org/10.1016/j.foodhyd.2016.08.002

820 Reis, P., Holmberg, K., Watzke, H., Leser, M. E., & Miller, R. (2009). Lipases at interfaces: a
821 review. *Advances in Colloid and Interface Science*, *147–148*, 237–250.
822 https://doi.org/10.1016/j.cis.2008.06.001

823 Reis, P. M., Raab, T. W., Chuat, J. Y., Leser, M. E., Miller, R., Watzke, H. J., & Holmberg, K.
824 (2008). Influence of surfactants on lipase fat digestion in a model gastro-intestinal
825 system. *Food Biophysics*, *3*(4), 370–381. https://doi.org/10.1007/s11483-008-9091-6

826 Reis, P., Miller, R., Leser, M., Watzke, H., Fainerman, V. B., & Holmberg, K. (2008). Adsorption
827 of polar lipids at the water−oil interface. *Langmuir*, *24*(11), 5781–5786.
828 https://doi.org/10.1021/la704043g

829 Reppas, C., Swidan, S. Z., Tobey, S. W., Turowski, M., & Dressman, J. B. (2009).
830 Hydroxypropylmethylcellulose significantly lowers blood cholesterol in mildly
831 hypercholesterolemic human subjects. *European Journal of Clinical Nutrition*, *63*(1), 71–
832 77. https://doi.org/10.1038/sj.ejcn.1602903

833 Reppas, Christos, Meyer, J. H., Sirois, P. J., & Dressman, J. B. (1991). Effect of
834 hydroxypropylmethylcellulose on gastrointestinal transit and luminal viscosity in dogs.
835 *Gastroenterology*, *100*(5), 1217–1223. https://doi.org/10.1016/0016-5085(91)70007-K

Sánchez, A., Maceiras, R., Cancela, A., & Rodríguez, M. (2012). Influence of n-hexane on in situ transesterification of marine macroalgae. *Energies*, *5*(2), 243–257. https://doi.org/10.3390/en5020243

Sarkar, N. (1995). Kinetics of thermal gelation of methylcellulose and hydroxypropylmethylcellulose in aqueous solutions. *Carbohydrate Polymers*, *26*(3), 195–203. https://doi.org/10.1016/0144-8617(94)00107-5

Slavin, J. L. (2005). Dietary fiber and body weight. *Nutrition*, *21*(3), 411–418. https://doi.org/10.1016/j.nut.2004.08.018

Staggers, J. E., Hernell, O., Stafford, R. J., & Carey, M. C. (1990). Physical-chemical behavior of dietary and biliary lipids during intestinal digestion and absorption. 1. Phase behavior and aggregation states of model lipid systems patterned after aqueous duodenal contents of healthy adult human beings. *Biochemistry*, *29*(8), 2028–2040. https://doi.org/10.1021/bi00460a011

The Dow Chemical Company. (2002). *METHOCEL cellulose ethers - Technical handbook*. (192-01062-0902 AMS), 1–32.

The Dow Chemical Company. (2013). Chemistry of METHOCEL™: cellulose ethers - a technical review. *METHOCEL™ - Technical Bulletin*, (198-02289-10/13 EST), 1–16. Retrieved from http://msdssearch.dow.com/PublishedLiteratureDOWCOM/dh_08e5/0901b803808e5f58.pdf?filepath=dowwolff/pdfs/noreg/198-02289.pdf&fromPage=GetDoc

Torcello-Gómez, A., Fernández Fraguas, C., Ridout, M. J., Woodward, N. C., Wilde, P. J., & Foster, T. J. (2015). Effect of substituent pattern and molecular weight of cellulose ethers on interactions with different bile salts. *Food and Function*, *6*(3), 730–739. https://doi.org/10.1039/c5fo00099h

Torcello-Gómez, A., & Foster, T. J. (2014). Interactions between cellulose ethers and a bile salt in the control of lipid digestion of lipid-based systems. *Carbohydrate Polymers*, *113*, 53–61. https://doi.org/10.1016/j.carbpol.2014.06.070

van der Gronde, T., Hartog, A., van Hees, C., Pellikaan, H., & Pieters, T. (2016). Systematic

review of the mechanisms and evidence behind the hypocholesterolaemic effects of HPMC, pectin and chitosan in animal trials. *Food Chemistry*, *199*, 746–759. https://doi.org/10.1016/j.foodchem.2015.12.050

Wilde, P. J., & Chu, B. S. (2011). Interfacial & colloidal aspects of lipid digestion. *Advances in Colloid and Interface Science*, *165*(1), 14–22. https://doi.org/10.1016/j.cis.2011.02.004

Wollenweber, C., Makievski, A. V., Miller, R., & Daniels, R. (2000). Adsorption of hydroxypropyl methylcellulose at the liquid/liquid interface and the effect on emulsion stability. *Colloids and Surfaces A: Physicochemical and Engineering Aspects*, *172*(1–3), 91–101. https://doi.org/10.1016/S0927-7757(00)00569-0

World Health Organization. (2019). Obesity and overweight. Retrieved June 26, 2019, from http://www.who.int/mediacentre/factsheets/fs311/en/

Younes, M., Aggett, P., Aguilar, F., Crebelli, R., Di Domenico, A., Dusemund, B., … Woutersen, R. A. (2018). Re-evaluation of celluloses E 460(i), E 460(ii), E 461, E 462, E 463, E 464, E 465, E 466, E 468 and E 469 as food additives. *EFSA Journal*, *16*(1), 1–104. https://doi.org/10.2903/j.efsa.2018.5047